Biophysical Journal, Volume 98

Supporting Material

A metabolite-sensitive, thermodynamically-constrained model of cardiac cross-bridge cycling: Implications for force development during ischemia

Kenneth Tran, Nicolas P. Smith, Denis S. Loiselle, and Edmund J. Crampin

Supporting Material S1 — A metabolite-sensitive, thermodynamically-constrained model of cardiac cross-bridge cycling: Implications for force development during ischemia

Kenneth Tran
Auckland Bioengineering Institute
University of Auckland, New Zealand

Nicolas P. Smith
University Computing Laboratory
University of Oxford, UK

Denis S. Loiselle
Auckland Bioengineering Institute
and Department of Physiology
University of Auckland, New Zealand

Edmund J. Crampin[1]
Auckland Bioengineering Institute
and Department of Engineering Science
University of Auckland, New Zealand

[1]Corresponding author: email: e.crampin@auckland.ac.nz

Rapid equilibrium binding of MgADP

In order to account for experimental observations on MgADP binding, we added a fifth state to the kinetic scheme, by expanding state $XBPostR$ into two force-producing sub-states, $AM1$ and $AM2$ (Fig. 1B, main text), where we assume that the two sub-states contribute equally to total force and MgADP is assumed to bind to state $AM1$. The five-state scheme can be made exactly equivalent to the four-state model when binding and unbinding of MgADP is rapid (states $AM1$ and $AM2$ are in rapid equilibrium), effectively reducing the five-state model to a four-state model as the rapid-equilibrium between $AM1$ and $AM2$ means that they can be treated as a single state. This allows the Extended Model to preserve the four-state structure of the original Rice et al. (1) model, and ensures that the original rate constants and parameters remain consistent and that the transient and steady-state properties are still reproducible.

In the following we derive the rapid equilibrium expressions for the binding of MgADP within the cross-bridge cycle. At steady-state, the rate of change between states $AM1$ and $AM2$ is zero (Fig. 1B):

$$AM1 \times [\text{MgADP}] \times k^{-} = AM2 \times k^{+} \tag{S1}$$

giving

$$\frac{AM2}{AM1} = \frac{[\text{MgADP}]}{k_{dADP}} \tag{S2}$$

where $k_{dADP} = \frac{k^{+}}{k^{-}}$, and:

$$AM1 + AM2 = XB_{PostR} \tag{S3}$$

Expressions for the occupancy of $AM1$ and $AM2$ can be written as fractions of XB_{PostR}:

$$AM1 = \frac{k_{dADP}}{k_{dADP} + [\text{MgADP}]} \times XB_{PostR} \tag{S4}$$

$$\tag{S5}$$

$$AM2 = \frac{[\text{MgADP}]}{k_{dADP} + [\text{MgADP}]} \times XB_{PostR} \tag{S6}$$

The apparent rate constants governing the transition away state XB_{PostR} is given by:

$$\begin{aligned} \alpha^{+} \times XB_{PostR} &= AM1 \times g^{*}_{xbT} \\ \alpha^{+} &= \frac{k_{dADP}}{k_{dADP} + [\text{MgADP}]} \times g^{*}_{xbT} \end{aligned} \tag{S7}$$

$$\begin{aligned} \alpha^{-} \times XB_{PostR} &= AM2 \times h^{*}_{bT} \\ \alpha^{-} &= \frac{[\text{MgADP}]}{k_{dADP} + [\text{MgADP}]} \times h^{*}_{bT} \end{aligned} \tag{S8}$$

where g^{*}_{xbT} and h^{*}_{bT} represent first order rate constants that *have* been adjusted to account for the assumption that the original Rice et al. (1) model is valid under normal metabolic conditions where the reference [MgADP] ($MgADP'$) is set to 36 uM. These rate constants are related to their respective equivalents (g_{xbT} and h_{bT}) from the original Rice et al. (1) by the following definitions:

$$g^{*}_{xbT} = \frac{k_{dADP} + MgADP'}{k_{dADP}} \times g_{xbT} \tag{S9}$$

$$h^{*}_{bT} = \frac{k_{dADP} + MgADP'}{MgADP'} \times h_{bT} \tag{S10}$$

Substituting Eq. S9 and S10 back into Eq. S7 and S8, respectively, yields the *apparent* MgADP-dependent rate constants:

$$\alpha^{-} = \frac{[\text{MgADP}]}{k_{dADP} + [\text{MgADP}]} \times \frac{k_{dADP} + MgADP'}{MgADP'} \times h_{bT} \tag{S11}$$

$$\alpha^{+} = \frac{k_{dADP}}{k_{dADP} + [\text{MgADP}]} \times \frac{k_{dADP} + MgADP'}{k_{dADP}} \times g_{xbT} \tag{S12}$$

These equations maintain the consistency between the parameters of our Extended Model and the parameters of the original Rice et al. (1) model such that under normal metabolic conditions when [MgADP] = $MgADP'$, $\alpha^{+} = g_{xbT}$ and $\alpha^{-} = h_{bT}$. By substituting the true first order rate constants for g_{xbT} and h_{bT} using Eqs. 3 and 6 the apparent rate constants in Eqs S11 and S12 are equivalent to Eqs. S18 and S20 (below), respectively.

Analysis of the inversion of the force-MgADP relationship

The trend-switching behaviour of the force-MgADP relationship is a function of placing the MgADP binding step between two strongly-bound force-producing states ($AM1$ and $AM2$). If we isolate the MgADP binding step, between these two states, from the rest of the cycle (such that we are only looking at a two-state model), it is obvious that isometric force will be independent of [MgADP] because $AM1 + AM2$ is conserved and isometric force is proportional to the summation of these two states. For example, increasing [MgADP] will decrease $AM1$ but $AM2$ will increase by a commensurate amount. But when placed in the context of the kinetic cross-bridge cycle, the populations of $AM1$ and $AM2$ are affected by all the other reactions in the cycle, particularly, the adjacent reactions. The trend of the

force-MgADP relation, depends on the balance between the competition for $AM1$ and $AM2$ sub-states. An increase in [Pi] or [H^+] will increase the transition away from $AM2$ and lead to a fall in the force-MgADP curve when [Pi] and [H^+] are greater than a certain threshold. Fig. S1 demonstrates the effect of changing [Pi] on the force-MgADP curve. When [Pi] increases above 5 mM, the force-MgADP relation reverses direction.

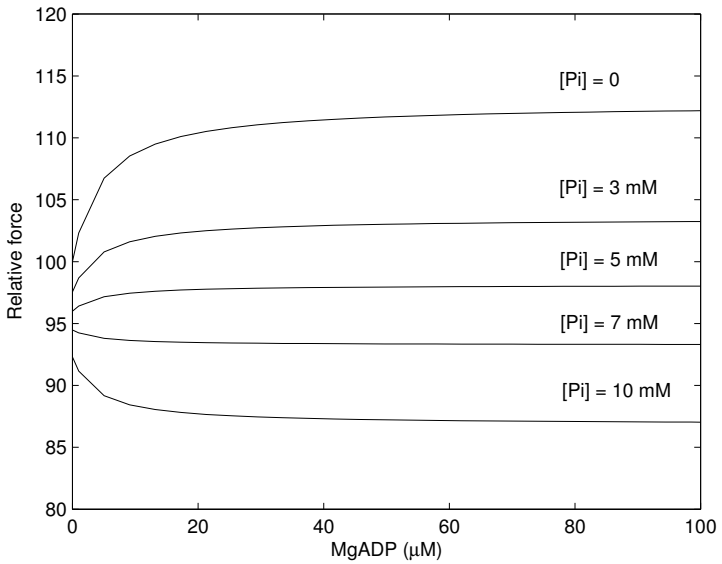

Figure S1: The force-MgADP relationship as a function of [Pi]. All curves are normalised to [MgADP] = 0 at [Pi] = 0. Other conditions in the simulation: [MgATP] = 1 mM, pH = 7, $[Ca^{2+}]_i$ = 100 uM (maximum activation), SL = 2.1 μm, T = 25 °C.

This behaviour appears to be consistent with the data of Shimizu et al. (2) showing a biphasic force response with increasing [MgADP]. Fig. S2 is a simulation of the observed biphasic behaviour where force initially increases with increasing [MgADP] but inverses and begins to decrease as [MgADP] is increased further. In this simulation, the conditions are set as outlined in the experiment and Pi concentration is assumed to increase commensurate with [MgADP]. As [Pi] increases, it causes a shift in the balance between states $AM1$ and $AM2$, tilting it towards state $AM2$ which signals the inversion and subsequent decline in force, similar to the behaviour observed in Fig. S1.

In modelling the MgADP binding step, we have chosen to model the two strongly-bound force-producing states, $AM1$ and $AM2$, as being of equal force. Mechanical

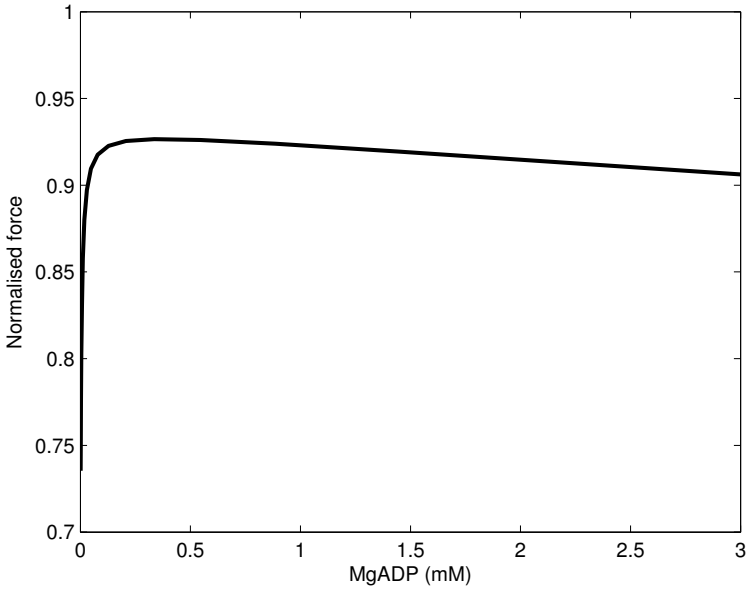

Figure S2: Normalised force as a function of MgADP demonstrating the biphasic force-MgADP relationship. Other conditions in the simulation: [MgATP] = 2 mM, pH = 7, $[Ca^{2+}]_i$ = 200 uM (maximum activation), SL = 2.1 μm, T = 25 °C.

measurements have shown that the binding of MgADP to attached myosin heads results in a small reduction in tension (3–6), indicating that state $AM2$ may not produce as much force as $AM1$. We have simulated this effect and found that it does not remove the reversal point (as the existence of the reversal point is independent of the relative force-bearing capacities of the two strongly-bound states), but would instead shift its position. But without experimental data to constrain this behaviour, the addition of an extra parameter to capture this effect is not warranted.

To rule out the possibility that this force-MgADP reversal behaviour is an artifact of the rapid equilibrium assumption, we have repeated the simulations shown in Fig. 3A in the full five-state model. The five-state model reproduces the force-MgADP reversal behaviour, demonstrating that this behaviour is independent of the rapid equilibrium assumption. A consequence of the rapid equilibrium construction is that the effect of [MgADP] on the force response changes very quickly at very low [MgADP] and saturates when [MgADP] is in the physiological range. This is consistent with the findings of Chase and Kushmerick (7) who specifically examined the effect of physiological concentrations of MgADP on the isometric force response and found it to be almost negligible.

In the following, we derive, and prove the existence of, the reversal point for the

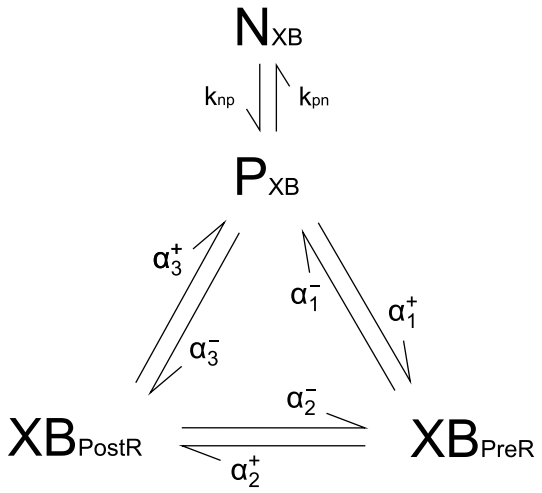

Figure S3: Schematic of the metabolite-sensitive extended model of cross-bridge kinetics.

effect of MgADP binding on isometric force development. The muscle is assumed to be under maximal Ca^{2+} activation, hence, only the states in the kinetic cycle, P_{XB}, XB_{PreR} and XB_{PostR} need to be considered. The cross-bridge scheme is reproduced in for convenience in Fig. S3, with the notation to be used in this derivation.

The time evolution of the occupancies of the three states can be described using two ordinary differential equations and one conservation equation (Fig. S3):

$$\frac{dXB_{PreR}}{dt} = \alpha_1^+ P_{XB} + \alpha_2^- XB_{PostR} - XB_{PreR}(\alpha_2^+ + \alpha_1^-) \quad \text{(S13)}$$

$$\frac{dXB_{PostR}}{dt} = \alpha_3^- P_{XB} + \alpha_2^+ XB_{PreR} - XB_{PostR}(\alpha_3^+ + \alpha_2^-) \quad \text{(S14)}$$

$$1 = P_{XB} + XB_{PostR} + XB_{PreR} \quad \text{(S15)}$$

where

$$\alpha_1^+ = f_{appT} \quad \text{(S16)}$$

$$\alpha_2^+ = h_{fT} \quad \text{(S17)}$$

$$\alpha_3^+ = [\text{MgATP}] \times g'_{xbT} \times \left(\frac{k_{dADP} + MgADP'}{k_{dADP} + [\text{MgADP}]} \right) \quad \text{(S18)}$$

and the apparent backward rate constants are defined as:

$$\alpha_1^- = [\text{Pi}] \times g'_{appT} \tag{S19}$$

$$\alpha_2^- = [\text{H}^+] \times h'_{bT} \times \left(\frac{k_{dADP} + MgADP'}{MgADP'} \times \frac{[\text{MgADP}]}{k_{dADP} + [\text{MgADP}]} \right) \tag{S20}$$

$$\alpha_3^- = f_{xbT} \tag{S21}$$

Since we are interested only in the steady-state occupancies of these states, we can set the time derivatives to zero and then solve the pair of coupled equations for the steady-state occupancies. Alternatively, this can also be achieved using the 'diagram method' which is particularly useful for large kinetic cycles (8). The steady-state probabilities are given below. The steady-state probability for P_{XB} is given for completeness but can be calculated from the probabilities of the other two states using the conservation equation (Eq. S15).

$$XB_{PreR} = \frac{\alpha_1^+\alpha_3^+ + \alpha_1^+\alpha_2^- + \alpha_2^-\alpha_1^-}{\Sigma} \tag{S22}$$

$$XB_{PosR} = \frac{\alpha_2^+\alpha_1^+ + \alpha_2^+\alpha_3^- + \alpha_3^-\alpha_1^-}{\Sigma} \tag{S23}$$

$$P_{XB} = \frac{\alpha_3^+\alpha_2^+ + \alpha_3^+\alpha_1^- + \alpha_2^-\alpha_1^-}{\Sigma} \tag{S24}$$

where

$$\begin{aligned} \Sigma = {} & \alpha_1^+\alpha_3^+ + \alpha_1^+\alpha_2^- + \alpha_2^-\alpha_1^- + \alpha_2^+\alpha_1^+ + \alpha_2^+\alpha_3^- + \\ & \alpha_3^-\alpha_1^- + \alpha_3^+\alpha_2^+ + \alpha_3^+\alpha_1^- + \alpha_2^-\alpha_1^- \end{aligned} \tag{S25}$$

The point at which the force-MgADP trend is neither increasing nor decreasing is characterized by complete insensitivity of force to [MgADP]. We can determine the conditions at which this point is produced by finding the rate of change of force with respect to [MgADP] and then setting this to zero.

$$\frac{dXB_{PostR}}{d[\text{MgADP}]} = 0 \tag{S26}$$

For an isometric steady-state simulation, the generated force is directly proportional to the occupancy of the strongly-bound state XB_{PostR}. The result is an equation that is *independent* of [MgADP]:

$$\begin{aligned} \frac{[\text{MgATP}]}{MgATP'} \times g_{xbT}\left(\frac{[\text{Pi}]}{Pi'} \times g_{appT} + f_{appT} + h_{fT}\right) = \\ \frac{k_{dATP}}{MgADP'} \times \frac{[\text{H}^+]}{H'} \times h_{bT} \times \left(\frac{[\text{Pi}]}{Pi'} \times g_{appT} + f_{appT} + f_{xbT}\right) \end{aligned} \tag{S27}$$

This equation relates all the other metabolite concentrations and all the reference concentrations to the kinetic parameters in the cross-bridge cycle and defines a family of curves at which force is invariant to [MgADP]. For example, for a given [Pi] and [H^+], we can rearrange Eq. S27 to calculate the [MgATP] at which the force is insensitive to [MgADP]:

$$\begin{aligned}[\text{MgATP}] \quad = \quad & \frac{h_{bT}}{g_{xbT}} \times \frac{k_{dADP}}{MgADP'} \times \frac{[\text{H}^+]}{H'} \\ & \times MgATP' \times \left(\frac{\frac{[\text{Pi}]}{Pi'} \times g_{appT} + f_{appT} + f_{xbT}}{\frac{[\text{Pi}]}{Pi'} \times g_{appT} + f_{appT} + h_{fT}} \right) \end{aligned} \quad \text{(S28)}$$

Similarly, the value of [Pi] at a given [MgATP] and [H^+] can be calculated using:

$$[\text{Pi}] = Pi' \times \left(\frac{\frac{k_{dADP}}{ADP'} \frac{[\text{H}^+]}{H'} h_{bT} \left(f_{appT} + f_{xbT}\right) - \frac{[\text{MgATP}]}{MgATP'} g_{xbT}(h_{fT} + f_{appT})}{g_{appT} \left(\frac{[\text{MgATP}]}{MgATP'} g_{xbT} - \frac{k_{dADP}}{MgADP'} \frac{[\text{H}^+]}{H'} h_{bT} \right)} \right) \quad \text{(S29)}$$

and the value of [H^+] at a given [MgATP] and [Pi]:

$$[\text{H}^+] = \frac{[\text{MgATP}]}{MgATP'} \times \frac{MgADP'}{k_{dADP}} \times \frac{g_{xbT}}{h_{bT}} \times H' \times \left(\frac{\frac{[\text{Pi}]}{Pi'} g_{appT} + f_{appT} + h_{fT}}{\frac{[\text{Pi}]}{Pi'} g_{appT} + f_{appT} + f_{xbT}} \right) \quad \text{(S30)}$$

Comparison of Force-Ca-pH curves to experimental data

Simulated pH-dependent force-Ca curves (as described in the main text) and experimental data from Orchard and Kentish (9) are shown in Fig. S4. The model derived pH-dependent force-Ca curves have a much steeper slope compared to the data from Orchard and Kentish (9). The steepness of the force-Ca curve represents the level of cooperativity within the non-linear Ca^{2+} activation process. The low extent of cooperativity implied by the Orchard and Kentish (9) data is a property of skinned muscle preparations which have been shown to be less sensitive to Ca^{2+} when compared to preparations from intact muscle fibres (10). This has been attributed to a number of factors including the lack of precise sarcomere length control, the difficulty in recreating the cytosolic environment of intact cells, and the swelling of the myofilament lattice brought about by the skinning

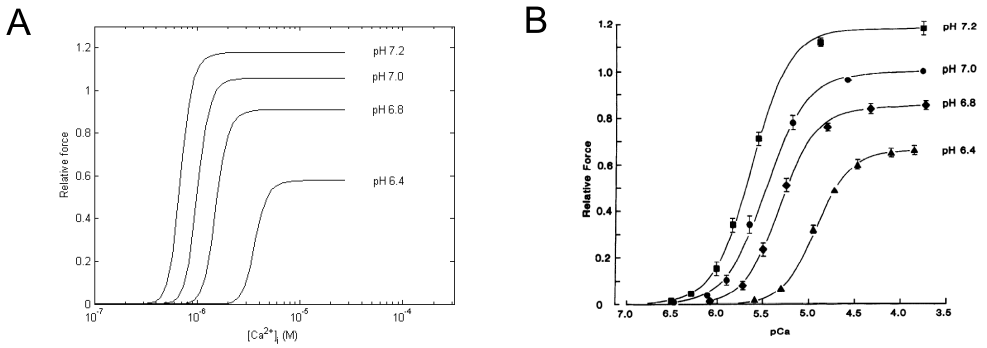

Figure S4: (***A***) Model simulation of steady-state force-Ca curves as a function of pH, as described in the text. (***B***) Experimental data reproduced from Orchard and Kentish (9) with permission from The American Physiological Society .

process (11, 12). Even with internal shortening enabled and set to about 20%, the cooperativity of the simulated model could be reduced only to 4. Further increases in internal shortening led to a dramatic fall in steady-state force (due to the force-length relation). For this reason, rather than trying to fit the force-Ca curves from the model directly to the Orchard and Kentish (9) data we have, instead, fitted the model to the relative change in the Ca^{2+} sensitivity of the force response, Ca_{50} (Fig. 2B).

Data selection

We used cardiac experimental data from a variety of sources to characterize the metabolic dependencies of the Extended Model. Consistent with our previous studies (13–15), we have used data from guinea pig cardiac tissue, where possible. The three parameters introduced in the Extended Model have been determined using data from guinea pig (k_{dHCa}, m) and rabbit cardiac tissue (k_{dADP}). We have, however, used data from rat for validating the behaviour of our model in response to changes in [MgATP] (Fig. 3C and D) to examine the qualitative behaviour of our model. This provides a possible explanation for the difference in time scale between the data in Fig. 3D and our simulations. For validating the qualitative behaviour of our model for both metabolic and sinusoidal length perturbations, we have used ferret cardiac data from Kawai et al. (16) (see Fig. S5 for sinusoidal length perturbation results for varying MgATP). The data that we have used to constrain our model parameters have been obtained at 22 °C (17) and 30 °C (9). We have accounted for this in the fitting process by setting the temperature-dependence of the Rice et al. (1) model to match those in the experiment.

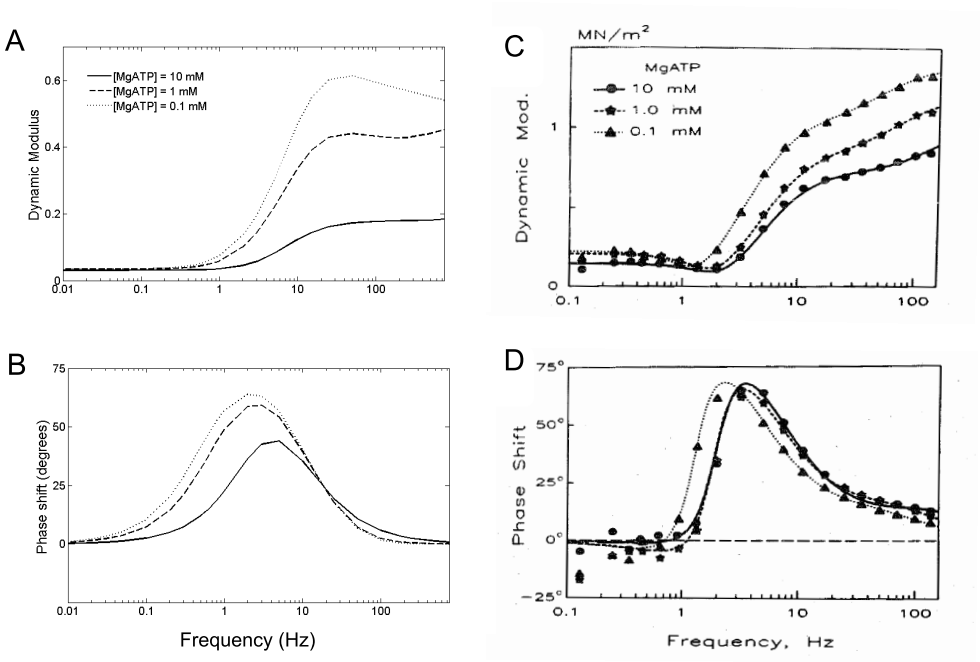

Figure S5: Sinusoidal Length Perturbations: Results for MgATP. Dynamic modulus and phase shift as a function of perturbation frequency and [MgATP], as referred to in the main text. Experimental data are from ferret cardiac muscle (reproduced from Kawai et al. (16) with permission from Wolters Kluwer Health). The dynamic modulus in the simulation is calculated from the amplitude of the normalised force oscillation in response to a sinusoidal length change protocol with an amplitude of 0.25% L_0 (where L_0 is set at 2.28 μm). Other conditions in the simulations: [Pi] =8 mM, [MgADP] = 0, pH = 7.15, [Ca^{2+}] = 200 uM and T = 20 °C. See main text for full details.

References

1. Rice, J. J., F. Wang, D. M. Bers, and P. P. de Tombe, 2008. Approximate model of cooperative activation and crossbridge cycling in cardiac muscle using ordinary differential equations. *Biophys J* 95:2368–2390.

2. Shimizu, H., T. Fujita, and S. Ishiwata, 1992. Regulation of tension development by MgADP and Pi without Ca^{2+} – role in spontaneous tension oscillation of skeletal-muscle. *Biophys J* 61:1087–1098.

3. Rodger, C. D., and R. T. Tregear, 1974. Crossbridge angle when ADP is bound to myosin. *J Mol Biol* 86:495–497.

4. Schoenberg, M., and E. Eisenberg, 1987. ADP binding to myosin cross-bridges and its effect on the cross-bridge detachment rate constants. *J Gen Physiol* 89:905–920.

5. Xu, S., J. Gu, S. Frisbie, and L. C. Yu, 1998. Structural changes in rigor (nucleotide-free) cross-bridges induced by the addition of MgADP. *Biophys J* 74:A363–A363.

6. Dantzig, J. A., M. G. Hibberd, D. R. Trentham, and Y. E. Goldman, 1991. Cross-bridge kinetics in the presence of MgADP investigated by photolysis of caged ATP in rabbit psoas muscle-fibers. *J Physiol* 432:639–680.

7. Chase, P. B., and M. J. Kushmerick, 1995. Effect of physiological ADP concentrations on contraction of single skinned fibers from rabbit fast and slow muscles. *Am J Physiol* 268:C480–C489.

8. Hill, T. L., 1989. Free Energy Transduction And Biochemical Cycle Kinetics. Springer-Verlag New York Inc.

9. Orchard, C. H., and J. C. Kentish, 1990. Effects of changes of pH on the contractile function of cardiac-muscle. *Am J Physiol* 258:C967–C981.

10. Gao, W. D., P. H. Backx, M. Azanbackx, and E. Marban, 1994. Myofilament Ca^{2+} sensitivity in intact versus skinned rat ventricular muscle. *Circ Res* 74:408–415.

11. Dobesh, D. P., J. P. Konhilas, and P. P. De Tombe, 2002. Cooperative activation in cardiac muscle: impact of sarcomere length. *Am J Physiol* 282:H1055–H1062.

12. Rice, J. J., and P. P. de Tombe, 2004. Approaches to modeling crossbridges and calcium-dependent activation in cardiac muscle. *Prog Biophys Mol Biol* 85:179–195.

13. Crampin, E. J., and N. P. Smith, 2006. A dynamic model of excitation-contraction coupling during acidosis in cardiac ventricular myocytes. *Biophys J* 90:3074–3090.

14. Terkildsen, J. R., E. J. Crampin, and N. P. Smith, 2007. The balance between inactivation and activation of the Na^+–K^+ pump underlies the triphasic accumulation of extracellular K^+ during myocardial ischemia. *Am J Physiol* 293:H3036–H3045.

15. Tran, K., N. P. Smith, D. S. Loiselle, and E. J. Crampin, 2009. A thermodynamic model of the cardiac sarcoplasmic/endoplasmic Ca^{2+} (SERCA) pump. *Biophys J* 96:2029–2042.

16. Kawai, M., Y. Saeki, and Y. Zhao, 1993. Crossbridge scheme and the kinetic constants of elementary steps deduced from chemically skinned papillary and trabecular muscles of the ferret. *Circ Res* 73:35–50.

17. Godt, R. E., and T. M. Nosek, 1989. Changes of intracellular milieu with fatigue or hypoxia depress contraction of skinned rabbit skeletal and cardiac-muscle. *J Physiol* 412:155–180.